Motion of Gas Bubbles in Non-Newtonian Liquids

GIANNI ASTARITA and GENNARO APUZZO

Istituto di Chimica Industriale, University of Naples, Naples, Italy

The available theoretical knowledge of the motion of gas bubbles in Newtonian liquids is reviewed, and the possibility of extension to non-Newtonian liquids, both purely viscous and viscoelastic, is studied. Experimental data on the rising velocities of gas bubbles in a variety of non-Newtonian liquids are presented and interpreted on the basis of theoretical knowledge. Peculiarities that have been observed in highly elastic liquids are discussed, and a tentative interpretation is offered.

The investigation of the motion of a gas bubble in a liquid presents theoretical problems of such remarkable complexity that rigorous solutions for the equations of motion are available only for a few limiting cases. Nonetheless, extension of these solutions to the non-Newtonian liquid case is not hopeless, and experimental data on terminal velocities of gas bubbles in non-Newtonian liquids are presumably of some interest.

The aim of this work is to investigate theoretically the motion of gas bubbles in non-Newtonian liquids, to present experimental data on terminal velocities, and to interpret the latter in the light of the theoretical knowledge available.

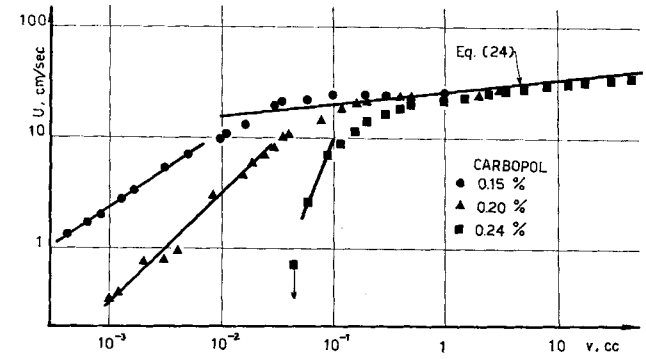

Fig. 1. Velocities in Carbopol solutions.

THEORY

Regimes of Motion

The conditions of motion of a gas bubble in a liquid are determined by three factors: the value of the Reynolds number, the shape of the bubble, and the interface characteristics.

At very low Reynolds numbers, creeping flow takes place in the liquid. The equations of motion can, in principle, be solved rigorously, provided the rheological equation of state of the liquid is known, and hence the drag can be calculated. By equating the drag to the buoyancy, the velocity-volume relationship can be obtained. It is important to point out that, in a Lagrangian sense, the flow in the liquid is not steady (the convected time derivatives are not zero), so that viscoelasticity may play an important role.

At very high Reynolds numbers, the motion in the bulk of the liquid follows the streamlines that can be calculated from inviscid flow theory. A boundary-layer solution may, in principle, allow the calculation of the drag; alternate ways of attacking the problem are through consideration of hydrodynamic forces, or by examination of the mechanism of energy dissipation. The problem of extending available solutions for Newtonian liquids to non-Newtonian liquids does not seem any more formidable than in the case of creeping flow.

The shape of a gas bubble is determined by hydrodynamic forces and by surface phenomena; the latter are unfortunately not simply those predictable from the concept of surface tension. Shapes observed in Newtonian liquids are sphere (at low enough volumes), oblate ellipsoid (at intermediate volumes), and spherical cap (at large volumes). Distortion from the simple spherical shape are discussed in references *12* and *35*.

The interface of a gas bubble may realize any condition between the two extreme cases of a *free* and of a *rigid* interface. A discussion of this point may be found in references *13*, *18*, and *21*. A free interface is one at which continuity of shear stress is satisfied, so that if the gas is assumed to be inviscid, the stress tensor τ is zero at a free interface. A rigid interface is such that the liquid velocity on it is everywhere equal to the velocity of the bubble's center of gravity.

The only known theoretical solutions for non-Newtonian liquids are relative to power-law liquids, which are characterized by the following rheological equation of state:

$$\tau = -\left\{ m \left| \sqrt{\frac{1}{2}\Delta : \Delta} \right|^{n-1} \right\} \Delta \qquad (1)$$

Available theoretical solutions are briefly reviewed in the following.

Stokes Regime. A gas bubble moves in the Stokes regime when the liquid is in creeping flow, the bubble is spherical, and the interface is rigid. These three conditions are satisfied for any liquid, provided the bubble volume is small enough (*1*, *6*).

The solution of the equations of motion for a Newtonian liquid for the case now considered was originally given by Stokes (*34*), and may be found in reference *30*. The drag coefficient is related to the Reynolds number through the equation

$$C_D = 24/N_{Re} \qquad (2)$$

and therefore the velocity of the bubble in the gravitational field U is related to the bubble volume by the equation

$$U = \frac{84.0}{\nu} v^{2/3} \qquad (3)$$

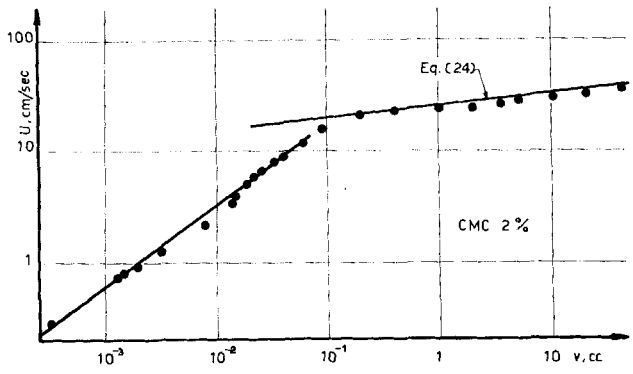

Fig. 2. Velocities in a CMC solution.

The analogous problem for power-law fluids has been studied extensively (*32, 36, 38, 40*). By definition of a modified Reynolds number

$$N'_{Re} = (2R)^n \rho U^{2-n}/m \tag{4}$$

it can be shown that the drag coefficient is given by

$$C_D = X_n/N'_{Re} \tag{5}$$

where X_n is a function of the flow index n. This function is not known rigorously, but only an upper and a lower bound have been calculated (*40*). The two bounds coincide at the value 24 when $n = 1$.

The velocity-volume relationship is

$$U = \left[\frac{\rho g}{m}\,\frac{2^{1+n}}{X_n}\left(\frac{4\pi}{3}\right)^{\frac{2-n}{3}}\right]^{\frac{1}{n}} v^{(1+n)/3n} \tag{6}$$

It is worthwhile pointing out that for pseudoplastic fluids ($n < 1$) the velocity U increases with increasing volume more rapidly than for Newtonian liquids.

$$n < 1, \quad \frac{d\log U}{d\log v} = \frac{1+n}{3n} > \frac{2}{3} \tag{7}$$

Hadamard Regime. A gas bubble moves in the Hadamard regime when the liquid is in creeping flow, the bubble is spherical, and the interface is free. These three conditions may for some liquids be impossible to realize simultaneously; for example, in liquids of low viscosity a bubble large enough to make the interface free may correspond to high Reynolds numbers. Water, and presumably also dilute aqueous solutions, presents conspicuous interfacial phenomena, which make doubtful the hypothesis of a free interface even for large bubbles (*7, 14, 26, 31, 33, 37*).

The equations of motion for the case considered have been solved independently by Hadamard (*15*) and by Rybczynsky (*28*). The drag coefficient is given by

$$C_D = 16/N_{Re} \tag{8}$$

and the bubble velocity by

$$U = \frac{126}{\nu} v^{2/3} \tag{9}$$

No solution for the analogous problem for non-Newtonian fluids has been published. Nonetheless, simple dimensional considerations show that for power-law fluids

$$C_D = X'_n/N'_{Re} \tag{10}$$

where X_n' is a function of n; the velocity is again given by Equation (6), where X_n' is substituted for X_n.

In fact, it is obvious that

$$\Delta \propto U/R \tag{11}$$

$$\tau \propto \rho g R \tag{12}$$

and since Equation (1) implies that in creeping flow

$$\tau \propto |\Delta|^n \tag{13}$$

the following is deduced:

$$U \propto R^{(1+n)/n} \tag{14}$$

Equation (10) is immediately obtained from Equation (14). Notice that (10) implies the validity of Equation (7).

Although a rigorous solution yielding the exact value of X_n' appears difficult, qualitative information on the characteristics of the function $X_n'(n)$ can easily be obtained. By analogy with a similar problem concerning a free interface phenomenon, which will be discussed in the following section, it is presumable that for pseudoplastic fluids

$$n < 1, \quad X_n' < 16 = (X_n')_{n=1} \tag{15}$$

On the other hand, it seems that the value of X_n in Equation (5) is larger than 24 (which is the value for Newtonian fluids), in agreement with all known solutions of boundary-layer problems for pseudoplastic fluids. Hence, presumably,

$$n < 1, \quad X_n/X_n' > 1.5 \tag{16}$$

The factor 1.5 is the ratio of the velocity in the Hadamard regime to the velocity in the Stokes regime for Newtonian fluids.

$$(U_{\text{Hadamard}}/U_{\text{Stokes}})_{n=1} = 1.5 \tag{17}$$

Consideration of Equations (6) and (16) shows that for pseudoplastic fluids

$$\left(\frac{U_{\text{Hadamard}}}{U_{\text{Stokes}}}\right)_{n<1} = \left(\frac{X_n}{X_n'}\right)^{\frac{1}{n}} > 1.5 \tag{18}$$

Levich Regime. A gas bubble moves in the Levich regime when the Reynolds number is high, the bubble is spherical, and the interface is free. These three conditions are theoretical, and may, for any given liquid, be impossible to realize simultaneously over a range of Reynolds numbers. In viscous liquids, a bubble large enough to make the Reynolds number large may have a shape that is severely distorted from spherical.

The investigation of the hydrodynamic conditions prevailing during the motion of gas bubbles at high Reynolds numbers is somewhat elusive (*16, 17, 20, 23, 25*). The streamlines in the bulk of the liquid are those that are

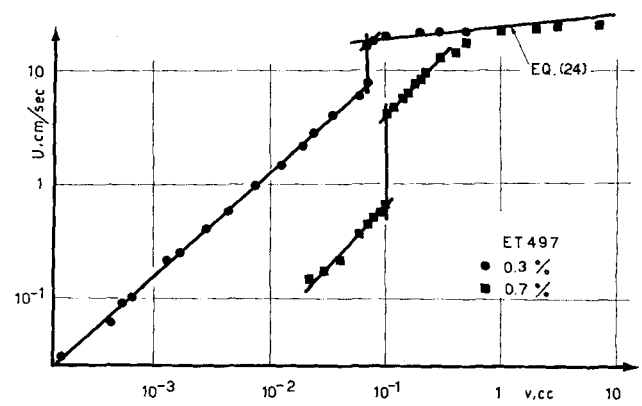

Fig. 3. Velocities in ET497 solutions.

calculated from inviscid flow theory; a very thin boundary layer develops in the vicinity of the interface in order to realize the condition $\Delta = 0$, which is required at a free interface (*8, 26*). Separation occurs very close to the lower pole (the usual separation condition, zero velocity gradient, is clearly not applicable in this case) so that a wake of negligible extent is formed. A rigorous solution has been obtained only recently by Moore (*26*), but Levich (*19*) should be credited for first obtaining the correct answer, although his reasoning is incorrect. The problem is solved by equating the viscous energy dissipation rate connected with the flow field calculated from inviscid flow theory to the rate of positional energy loss due to the motion of the gas bubble. The drag coefficient is given by

$$C_D = 48/N_{Re} \tag{19}$$

and hence the velocity U is given by

$$U = \frac{42.0}{\nu} v^{2/3} \tag{20}$$

The solution has been extended to power-law fluids by Astarita and Marrucci (2); the drag coefficient is in this case given by

$$C_D = K_n/N'_{Re} \tag{21}$$

where

$$K_n = \frac{2^{n+3}\,3^{n+1}}{1+4n} \int_0^1 (1+2x^2)^{(n+1)/2}\,dx \tag{22}$$

The function $K_n(n)$ takes values, which, for $n < 1$, are always smaller than 48. This point justifies the assumption of inequality (15) in the analogous free interface problem.

The velocity U is related to the volume v by Equation (6), with K_n substituted for X_n.

Taylor Regime. A gas bubble moves in the Taylor regime when the Reynolds number is high, the bubble has a spherical cap shape, and the interface is free. Abundant experimental evidence (*9, 14*) permits the assumption that these conditions are realized in any liquid, provided the volume of the bubble is large enough.

Simple dimensional considerations show that in the Taylor regime, the velocity U is proportional to the 1/6 power of the bubble volume (9). Moore (25) has shown, through simple consideration of the hydrodynamic forces involved, that

$$U = \frac{2}{3}(gR')^{1/2} \tag{23}$$

where R' is the curvature radius of the cap. Of course, Equation (23) does not give any information on the relationship between U and v, unless the angle θ of the cap is known.

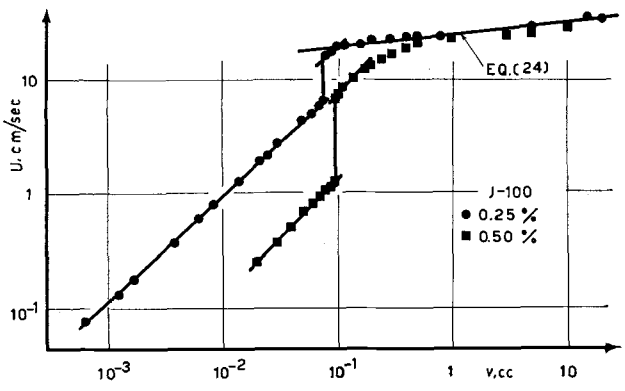

Fig. 4. Velocities in J-100 solutions.

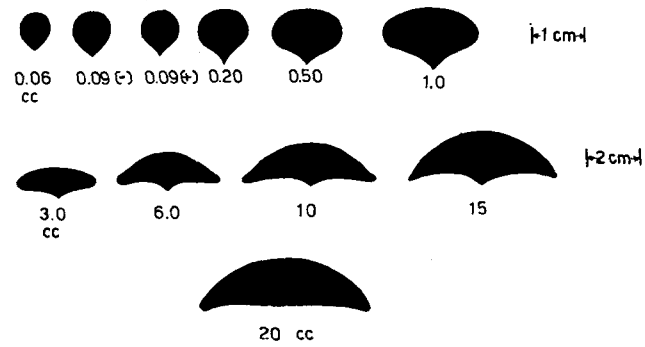

Fig. 5. Shape of bubbles in a 0.5% J-100 solution.

Moore (25) has tried to solve the problem theoretically by assuming the existence of an infinite wake. This, of course, avoids the difficulty of balancing the energy dissipation rate with the rate of potential energy loss; Moore calculates for θ a value of 39 deg. In contrast to this, Davies and Taylor (9) give evidence of an approximately spherical turbulent wake, and of a value of about 50 deg. for θ. Astarita and Apuzzo (5) have made accurate measurements of θ, and again indicate a value of 50 deg. By using the latter value, Equation (23) yields

$$U = 25.0\ v^{1/6} \tag{24}$$

which corresponds to a value 2.6 for the drag coefficient, as compared to 2.1 calculated by Moore. Equation (24) is in excellent agreement with all available data (*9, 14*) relative to Newtonian liquids.

Although the liquid viscosity does not enter into Equation (23), one cannot rule out the possibility that the rheological properties of the liquid influence the value of the coefficient in Equation (24). In fact, if the energy dissipates in the turbulent wake behind the bubble, the ultimate mechanism of dissipation is viscous dissipation, and it is conceivable that in a power-law fluid, for example, the angle θ may be a function of the flow index n. [For a discussion of the mechanism of turbulent energy dissipation in a non-Newtonian purely viscous liquid, see Lumley (22).] Still more complex to investigate is the case of a viscoelastic liquid, in which the turbulent energy dissipation mechanism may be anomalous (*3, 4, 10*).

EXPERIMENTAL

Data on terminal velocities of gas bubbles have been collected for four types of non-Newtonian solutions:

1. Aqueous solutions of Carbopol. Previous rheological data showed that these are presumably purely viscous, highly pseudoplastic liquids.
2. Aqueous solutions of carboxymethylcellulose (CMC). These solutions are slightly elastic; in steady shear, the rheological behavior is almost Newtonian at low shear rates.
3. Aqueous solutions of ET497 (a commercial additive). These solutions are highly elastic; in steady shear they display pseudoplastic behavior.
4. Aqueous solutions of J-100 (a commercial additive). The rheological behavior is analogous to that of ET497 solutions.

The shape of the gas bubbles has been investigated by means of a photographic technique, which proved to be satisfactory only for the ET497 and J-100 solutions; in the Carbopol and CMC solutions, although good photographs could be taken, from which the shape of the bubbles could be ascertained qualitatively, no quantitative geometrical data could be obtained because of unavoidable blurring of the bubble's contour. Fortunately the shape of gas bubbles in the two highly elastic liquids proved to be particularly interesting, as discussed below.

Figures 1 to 4 are plots of the terminal velocity U vs. the bubble volume v for the four types of non-Newtonian solutions that were studied. Figure 5 illustrates the shape of

the vertical cross section of the bubbles in the 0.5% J-100 solution. Original data, as well as a complete description of the experimental technique, are reported in reference 28.

DISCUSSION

Large Volume Bubbles

In Figures 1 to 4 the line corresponding to Equation (24) is plotted. The data clearly show that at large enough volumes, the conditions of the Taylor regime are satisfied for all the liquids. A coefficient slightly lower than 25.0 would appear to correlate the non-Newtonian data somewhat better, which is not in contrast with theory.

A value of θ of about 50 deg. would correspond to the following relationship among the curvature radius R' and the bubble volume:

$$R' = 1.44\ v^{1/3} \qquad (25)$$

which yields Equation (24) when inserted into Equation (23). Values of R' have been accurately measured from the photographs for the spherical cap bubbles in the two J-100 solutions. The measured values are indeed proportional to the cubic root of the bubble volume (hence θ is independent of v), but the proportionality factor is slightly less than 1.44, and appears to depend on the non-Newtonian character of the liquid.

$$0.25\%\ \text{J-100}\ , \qquad R'\,v^{-1/3} = 1.19$$

$$0.50\%\ \text{J-100}\ , \qquad R'\,v^{-1/3} = 1.03$$

These results agree perfectly with the fact that the terminal velocity, although proportional to the sixth root of the volume, is slightly less than predicted by Equation (24).

It is worthwhile to point out that although all large volume bubbles observed have the shape of a spherical cap, a peculiarity exists in the case of highly elastic liquids (ET497 and J-100). The lower surface of the bubble presents a clearly visible protruding tip at the center, so that the vertical cross section appears to have the shape that is sketched in Figure 5.

Small Volume Bubbles

Let us first examine the data for purely viscous (Figure 1) and for moderately elastic (Figure 2) liquids. It is seen that condition 7 is fulfilled in every case. The values of the slope of the log U-log v curve, as well as the apparent flow indexes that are calculated from these slopes, are reported in Table 1.

In the last column of Table 1, the values of n obtained from capillary-viscometer data for the same fluids are reported. It is seen that good agreement exists between the two sets of n values, possibly with the exception of the 0.24% Carbopol solution. It should be mentioned that this solution seems to approximate the Bingham fluid behavior (for a Bingham fluid, the apparent value of n strongly depends on the shear rate, approaching zero at low shear rates). In fact, bubbles of volume smaller than 0.045 cc. did not move at all in this solution ($U = 0$), which means that the liquid, at low enough shear stresses, behaves as a solid (in a solid, a gas bubble may be incorporated indefinitely). The agreement between the n values calculated from the U vs. v plots with those obtained from the capillary viscometer data shows that in these solutions, there are no conspicuous elastic effects. In fact, a rheological parameter calculated from steady shear data (such as in a capillary viscometer) correlates results in a flow field where the convected derivatives are not zero (such as in the liquid surrounding a gas bubble).

Table 1. Purely Viscous and Moderately Elastic Liquids

Solution	$\frac{d \log U}{d \log v}$	n	n, from capillary viscometer (shear rate range: $10^4 \div 10^5$ sec.$^{-1}$)
0.15% Carbopol	0.70	0.910	0.92
0.20% Carbopol	1.0	0.500	0.56
0.24% Carbopol	2.6	0.147	0.32
2.0% CMC	0.74	0.82	0.80

The shape of the gas bubbles in the Carbopol and CMC solutions is the usual shape, which passes from spherical to oblate ellipsoid to spherical cap.

The velocity-volume curve in the highly elastic liquids shows a striking peculiarity: a critical volume exists, v_c, corresponding to an abrupt increase in the velocity, by a factor which may be as large as 6 (see Figures 3 and 4). The phenomenon is clearly visible in all curves; the increase factor for velocity appears to be larger when the slope of the log U-log v curve is larger. The bubble shape is also unexpected; it is clearly prolate, and the lower pole is markedly cuspidal (see Figure 5). The shape of the bubble also seems to undergo a transition, although not very marked, at the critical volume when $v < v_c$, although the rear pole is cuspidal, the whole bubble's surface appears to be convex. In contrast to this, when $v > v_c$, the protruding tip at the rear pole is more marked, and the bubble's surface appears to be concave along an horizontal circle slightly above the protruding tip. It is worthwhile mentioning that in the case of spherical caps, the presence of a tip implies the existence of a concave region on the bubble's surface.

A possible interpretation of the phenomenon described above is tentatively presented in the following.

We shall assume that the observed transition is due to a transition from the Stokes to the Hadamard regime, and that viscoelasticity is responsible for the abruptness of the transition.

In favor of this interpretation is the fact that the slope of the log U-log v curve is the same for volumes smaller

Table 2. Highly Elastic Liquids

Solution	$\left(\frac{d \log U}{d \log v}\right)_{v=v_c}$	Velocity increase factor, $\left(\frac{U_{\text{Hadamard}}}{U_{\text{Stokes}}}\right)_{v=v_c}$	$n_{v=v_c}$	n, from capillary viscometer (shear rate range as in Table 1)
Newtonian	0.667	1.500	1.00	1.00
0.30% ET497	0.93	2.22	0.56	0.88
0.25% J-100	0.94	2.35	0.55	0.85
0.50% J-100	1.06	5.55	0.46	0.73
0.70% ET497	1.10	5.86	0.43$_5$	0.72

and larger than v_c, and the discussion leading to Equation (18). In fact, an increase of velocity by a factor larger than 1.5, and increasing with increasing pseudoplasticity, would be required in order to explain the results on the basis of a transition from the Stokes to the Hadamard regime. Indeed such an increase factor has been observed. Table 2 gives the values of the velocity increase factor observed at $v = v_c$, as well as the local values of $d \log U/d \log v$, and of the apparent flow index calculated from the latter. Although two different solutions are considered, the increase factor appears indeed to be an unique function of the apparent flow index, as Equation (18) would predict. Furthermore, the existence of a concave region on the bubble's surface, which has been ascertained in the Taylor regime, and which is observed only at $v > v_c$, is in favor of the existence of a free interface at volumes larger than the critical volume.

In the last column of Table 2 the values of n obtained at the capillary viscometer for the same solutions are reported. It is clear that in this case the two sets of n values do not agree with each other. In other words, the slope of the log U-log v curve is higher than would be predicted by Equation (7) on the basis of rheological data taken under conditions of steady shear. The difference is larger than could be attributed to a difference in the shear stress range (and of opposite direction). Therefore, it is presumable that the difference should be attributed to viscoelasticity, which does not affect the steady shear data, but plays a role in the motion of gas bubbles.

A steep, although not abrupt, increase in velocity at some critical volume has also been observed in the case of liquid drops moving through non-Newtonian liquids (*11, 24, 39*). Warshay et al. (*39*) propose that the increase in velocity is due to the start of internal circulation within the drop (which is equivalent to a transition from the Stokes to the Hadamard regime), and to a change of shape causing a smaller frontal area. The second effect does not apply in our case. The results of an accurate photographic investigation of the shape of gas bubbles in the 0.5% J-100 solution, which are given in Figure 5, clearly show that the frontal area of a bubble just above the transition, 0.09(+), is not smaller but probably larger than the frontal area of a bubble just below the transition, 0.09(−). Dr. Kintner has kindly sent us enlarged copies of his photographs of liquid drops falling through non-Newtonian liquids, and the same observation seems to hold true also in the case of liquid drops.

The data of Kintner and co-workers (*24, 39*) confirm the interpretation given here in another respect. Figure 2 of reference *24* and Figure 7 of reference 39 show an increase factor for velocity of about 1.7. The continuous phase was in both cases a concentrated CMC solution with a limiting viscosity of 463 cp., which Faraoui and Kintner (*11*) indicate as having a flow index of 0.806. The couple of values 1.7 for the velocity increase factor and 0.806 for n could well be inserted as the second line of Table 2, thus confirming the interpretation given here, namely that the velocity increase is due to a transition from the Stokes to the Hadamard regime. The fact that the effect discussed above, which has been attributed to viscoelasticity, has been observed in CMC solution, should not be surprising, since these solutions are known to be moderately elastic. The CMC solution used in this work was less concentrated, and presumably of lower molecular weight, than the one used by Kintner.

A transition from the Stokes to the Hadamard regime may be observed also in Newtonian liquids (*13*); for example, Figure 6 is a plot of U vs. v for a concentrated glycerol solution, where the transition is observed at a volume of about 0.008 cc. But in this case the transition is not abrupt, nor are the peculiar shapes reported in Figure 5 observed. Therefore, viscoelasticity should be considered as playing an important role.

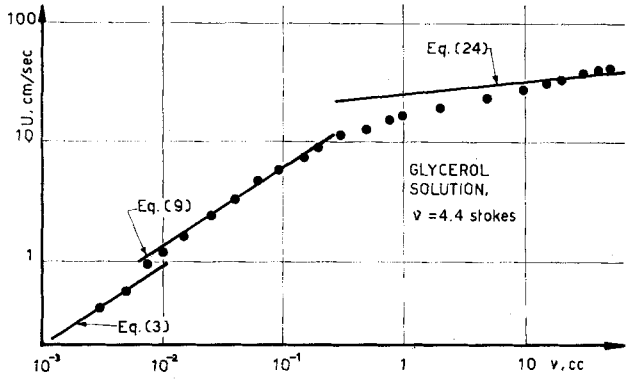

Fig. 6. Velocities in a concentrated glycerol solution.

NOTATION

C_D = drag coefficient, = $8gR/3U^2$, dimensionless
g = gravity acceleration, = 981 cm. sec.$^{-2}$
h = vertical length of bubble, cm.
K_n = coefficient in Equation (21), dimensionless
m = consistency, g. cm.$^{-1}$ sec.$^{n-2}$
n = flow index, dimensionless
R = equivalent radius, = $(3v/4\pi)^{1/3}$, cm.
R' = curvature radius, cm.
N_{Re} = Reynolds number, dimensionless, = $2RU/\nu$
N'_{Re} = Reynolds number, dimensionless, = $(2R)^n U^{2-n} \rho/m$
U = velocity of bubble, cm. sec.$^{-1}$
v = volume of bubble, cc.
v_c = critical volume, cc.
x = dummy variable, dimensionless
X_n = coefficient in Equation (5), dimensionless
X_n' = coefficient in Equation (10), dimensionless

Greek Letters

Δ = shear rate tensor, sec.$^{-1}$
θ = angle of spherical cap, dimensionless
ν = kinematic viscosity, sq.cm. sec.$^{-1}$
ρ = density of the liquid, g. cm.$^{-3}$
τ = stress tensor, g. cm.$^{-1}$ sec.$^{-2}$

LITERATURE CITED

1. Arnold, H. D., *Phil. Mag.*, **22**, 755 (1911).
2. Astarita, Gianni, and G. Marrucci, *Rend. Cl. Sci. Fis. Mat. Natl. Accad. Lincei*, **8-36**, 836 (June, 1964).
3. ———, *Chim. Ind. (Milan)*, **46**, 910 (1964).
4. ———, *Ind. Eng. Chem. Fund.*, in press.
5. ———, and Gennaro Apuzzo, *Chim. Ind. (Milan)*, **45**, 1059 (1963).
6. Bond, W. N., and D. A. Newton, *Phil. Mag.*, **5**, 793 (1924).
7. Boussinesq, J., *Compt. Rend.*, **156**, 113 (1924).
8. Chao, B. T., *Phys. Fluids*, **5**, 69 (1962).
9. Davies, R., and G. I. Taylor, *Proc. Roy. Soc. (London)*, **A-200**, 375 (1950).
10. Dodge, D. W., Ph.D. thesis, Univ. Delaware, Newark (1957).
11. Fararoui, A., and R. C. Kintner, *Trans. Soc. Rheol.*, **5**, 369 (1961).
12. Frunkin, A. N., and V. G. Levich, *Zh. Fiz. Khim.*, **21**, 1183 (1947).
13. Garner, F. H., and D. Hammerton, *Chem. Eng. Sci.*, 3, 1 (1954).
14. Habermann, W. L., and R. K. Morton, *Trans. Am. Inst. Civil Engr.*, **121**, 227 (1956).
15. Hadamard, J., *Compt. Rend.*, **152**, 1735 (1911).

16. Hartunian, R. A., and W. R. Sears, *J. Fluid Mech.*, 3, 27 (1957).
17. Ladyzhenskij, R. M., *Zh. Prikl. Khim.*, **27**, 17 (1954).
18. Levich, V. G., "Physico-Chemical Hydrodynamics," Prentice-Hall, Englewood Cliffs, N. J. (1962).
19. ———, *Zh. Eksp. Teoret. Fiz.*, **19**, 18 (1949).
20. Lochiel, A. C., Ph.D. thesis, Univ. Edinburgh, Scotland (1963).
21. ———, and P. H. Calderbrank, *Chem. Eng. Sci.*, **19**, 471 (1964).
22. Lumley, T. J., *Phys. Fluids*, **7**, 335 (1964).
23. Marrucci, G., and B. T. Chao, personal correspondence (1963).
24. Mhatre, M. V., and R. C. Kintner, *Ind. Eng. Chem.*, **51**, 865 (1959).
25. Moore, D. W., *J. Fluid Mech.*, **6**, 113 (1959).
26. ———, *ibid.*, **16**, 161 (1963).
27. Orell, A., and J. W. Westwater, *Chem. Eng. Sci.*, **16**, 127 (1961).
28. Rybzcynsky, W., *Bull. Acad. Cracovia*, **A-40** (1911).
29. Sandulli, E., *Lab. Notebook Univ. Naples* (1964).
30. Schlichting, H., "Boundary Layer Theory," McGraw-Hill, New York (1964).
31. Sherwood, T. K., and J. C. Wei, *Ind. Eng. Chem.*, **49**, 1030 (1957).
32. Slattery, J. C., *A.I.Ch.E. J.*, **8**, 663 (1962).
33. Sternling, C. V., and L. E Scriven, *ibid.*, **5**, 514 (1959).
34. Stokes, G. G., "Mathematical and Physical Papers," Cambridge Univ. Press, England (1880).
35. Taylor, T. D., and A. Acrivos, *J. Fluid Mech.*, **18**, 466 (1964).
36. Tomita, Y., *Bull. Soc. Mech. Engrs.*, **2**, 469 (1959).
37. Valentine, R. S., and W. J. Heidiger, *Ind. Eng. Chem. Fundamentals*, **2**, 242 (1963).
38. Wallick, G. C., J. G. Savins, and D. R. Atterburn, *Phys. Fluids*, **5**, 367 (1962).
39. Warshay, H., E. Bogusz, M. Johnson, and R. C. Kintner, *Can. J. Chem. Eng.*, **37**, 29 (1959).
40. Wassermann, M. L., and J. C. Slattery, paper presented at A.I.Ch.E. Houston meeting (1963).

Manuscript received February 25, 1965; revision received April 29, 1965; paper accepted April 30, 1965.

Ion Flotation of Dichromate with a Cationic Surfactant

ROBERT B. GRIEVES, THOMAS E. WILSON, and KENNETH Y. SHIH

Illinois Institute of Technology, Chicago, Illinois

An experimental investigation is presented of the flotation of dichromate ion from aqueous solution with a cationic surfactant, ethylheaxadecyldimethylammonium (EHDA) bromide. Dichromate forms a colloidal complex with EHDA ion in a molar ratio of approximately 1 : 2. Excess surfactant causes the formation of a stable foam to which the complex is adsorbed, providing the separation of dichromate from aqueous solution. Batch flotation studies were conducted utilizing approximately 2-liter solutions containing from 10 to 200 mg. of dichromate ion (4.8 to 96.3 mg. of hevavalent chromium), with masses of EHDA-Br ranging from 400 to 800 mg. The effects of mass of surfactant added, dichromate concentration, pH, and possible interfering anions were determined. A comparison is made with pure surfactant solutions, and the mechanism of the process is discussed.

Most efficient operation is achieved with a molar feed ratio of EHDA ion to dichromate ion from 2.1 to 3.0, and removal ratios ranging from 80 to 95% are obtained. Reduction of the residual dichromate below 10% of the feed concentration requires additional surfactant and produces excessive foam, which could be overcome by modifications in operating conditions.

Ion flotation (foam separation) has been utilized by chemists and chemical engineers for the removal and separation of inorganic and organic cations and anions from aqueous solution. The process involves the addition of a surface-active agent to the solution; a complex between the anion or cation and the surfactant is formed, or the mechanism involves the electrostatic attraction between the surfactant ion and the ion to be concentrated. The complex may be floated to the surface of the solution by means of gas bubbles to the interfaces of which it is adsorbed and a froth may be formed. If the complex is insoluble in water and a scum is formed at the solution-froth interface, the process may be termed ion flotation. The insoluble complex may be removed from the surface of the solution as a froth if low gas flow rates are employed; or it may be carried into a tall column of foam if high gas flow rates are employed. The latter mode of operation provides more effective removal of excess quantities of the surface-active agent. The mechanism of the process involves the flotation of colloidal size particulates. An extensive discussion and review of applications have been presented by Sebba (*8*). If the complex is soluble and further enrichment is obtained in the foam phase, or if the process involves electrostatic ion attraction, it may be termed foam separation. A review of foam separation, including an excellent discussion on metal ions, has been presented by Rubin and Gaden (*5*). The most extensive engineering application has been made to the concentration of cations from radioactive waste solutions (*4, 6, 7*).

Hexavalent chromium in the form of chromate and/or dichromate is found in varying quantities in a multiplicity of industrial wastes. Most are wastewaters from metal finishing industries concerned with the cleaning of metals or with the coating of them with chromium. Chromic acid is used in plating plants for several purposes, including plating solutions, anodizing solutions, chromating solutions, and paint pretreatment solutions. Although the con-